Computational Study of the Vortical Flow over a Yawed LEX-Delta Wing at a High-Angle of Attack

Tae-Ho Kim, Yong-Hun Kweon, Heuy-Dong Kim and Myong-Hwan Sohn

고영각 Yawed LEX-Delta 익에서 발생하는 와유동의 수치해석

김태호* • 권용훈* • 김희동† • 손명환**

Key Words : Delta Wing(델타익), Leading Edge Extension(LEX), Vortex Breakdown(와붕괴), Wing Aerodynamics(익형 공기역학)

Abstract

The vortex flow characteristics of a yawed LEX-delta wing at a high-angle of attack are studied using a computational analysis. The objective of the present study is to investigate and visualize the effects of the yaw angle, the development and interaction of vortices, the relationship between the suction pressure distributions and the vortex flow characteristics. Computations are applied to the three dimensional, compressible, Navier-Stokes Equations. In computations, the yaw angle is varied between 0 and 20 degree at a high-angle of attack. Computational predictions are compared with the previous experimental results.

1. INTRODUCTION

Many modern combat or supersonic airplanes which are required a high maneuverability performance have adopted the delta wing which have ability to minimize the influence of the shock wave generated in the vicinity of the sound speed area and to maintain stability at the moment of supersonic aviation. Many problems exist with regard to sudden reduction of maneuverability and generation of induced drag at low speed area, difficulty in use of high-lift device and requirement of high-angle of attack at takeoff or landing owing to stall generation, etc.[1, 4]. The vast majority of delta-winged aircraft spends a great deal of their flight time at subsonic speeds. For this reason, the low-speed aerodynamic characteristics of delta wings are also of great importance. Therefore, the low-speed aerodynamics of delta wings has been a subject of much study.

When a flow approaches a delta wing pitched at certain angle of attack with subsonic speed, two spiraling vortices are formed as the flow separates into pair of shear layers at the leading edges. These vortices increase their size as they are convected downstream by the free stream velocity of the outer flow.

These wing vortices generated at the surface of delta wing by the flow separation increase the lift and maneuverability performance of flight. With an increase in the angle of attack, however, they are strengthened, and the resulting lift of the delta wing increases until a critical angle of attack is reached, where the vortices break down and periodic vortex shedding effect resulting in a dramatic loss of lift, a sudden change of pitching moment and buffeting.

So far, the aerodynamic community of the countries having advanced aerospace technology has been paid a lot of efforts to understand, to predict and control the vortex flows over those components and the effects of them upon the high angle of attack characteristics. Grismer, Harbbar, Erickson, Verhaagen et al. [1-3] investigated experimentally regarding the vortex generation, break down and interactions with shock wave on the delta wing at subsonic, transonic and super sonic speeds. Ekaterinaris, Hue, Liu, Kern, Craig et al. [4-6] performed computationally about the vortex control at a high angle of attack of delta wing.

† 안동대학교 기계공학과
E-mail : kimhd@andong.ac.kr
TEL : (054)820-5622 FAX : (02)123-1234
* 안동대학교 원 기계공학과
** 공군사관학교 항공우주공학과

The present study investigates numerically and experimentally the vortex flow characteristics of a sharp-edged delta wing with a leading edge extension according to the variation of yaw angle. In computations, the yaw angle is varied between 0 and 20 degree and the free stream velocity is fixed in 20m/s. The results obtained from the present computations are compared with the experimental ones and visualize path line, density contour, total pressure contour, vorticity, particle trajectory etc. which are hardly disclosed by experimental work.

2. NUMERICAL METHOD

2.1 Governing Equations

The governing equations are mass averaged, compressible, implicit 3D Navier-Stokes equations. The resulting equations are as follows

$$\frac{\partial r}{\partial t}+\frac{\partial}{\partial x_i}(ru_i)=0$$

$$\frac{\partial}{\partial t}(ru_i)+\frac{\partial}{\partial x_j}(ru_iu_j)=\frac{\partial}{\partial x_j}m\left(\frac{\partial u_i}{\partial x_j}+\frac{\partial u_j}{\partial xx_i}\right)-\frac{\partial}{\partial x_i}\left(\frac{2}{3}m\frac{\partial u_l}{\partial x_l}\right)$$

$$-\frac{\partial p}{\partial x_i}+\frac{\partial}{\partial x_j}(-r\overline{u_i'u_j'})$$

$$\frac{\partial}{\partial t}(rE)+\frac{\partial}{\partial x_i}(ru_iH)=\frac{\partial}{\partial x_i}\left[\left(x+\frac{m_t}{\mathrm{Pr}_t}\right)\frac{\partial T}{\partial x_i}+u_j(t_{ij})_{eff}\right]$$

The governing equations are discretized spatially implicit finite volume scheme. With respect to temporal discretization, explicit 4-stage Runge-Kutta time stepping scheme is used. Used turbulence model is standard k-e turbulent model which is a semi-empirical model based on model transport equations for the turbulence kinetic energy(k) and its dissipation rate(e).

2.2 Computational Domain and Grid System

Fig.1 shows the schematic diagram of the delta wing model used in this study. The wing model is a flat type wing having LEX. It has the 65^o sweepback angle with 600mm root chord, 15mm thickness 475.4 mm span at the trailing edge. In this study, the coordinate system is Cartesian coordinates. x is the coordinate along the wing centerline, measured from the wing apex, y is the coordinate along the wing span measured from the wing centerline, and z is the coordinate normal to the wing upper surface. The origin of the coordinate system is the apex of the delta wing. In the computations, the yaw angle of the delta wing rages from 0 to 20 degree. The free stream velocity is fixed in 20m/s. For comparison with experimental results, computational data were acquired at the location of 30%, 45%, 60%, 80% of chord length.

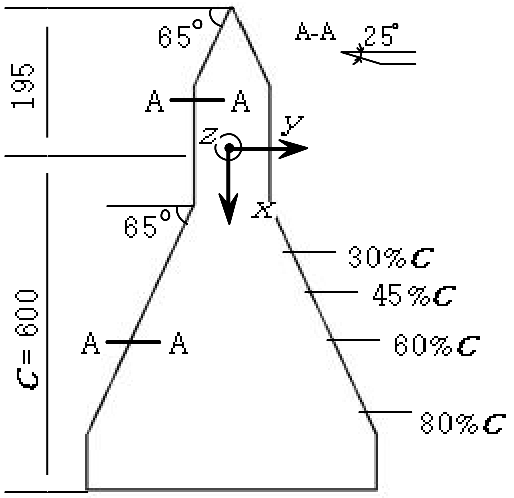

Fig. 1 Schematic diagram of delta wing used (unit:mm)

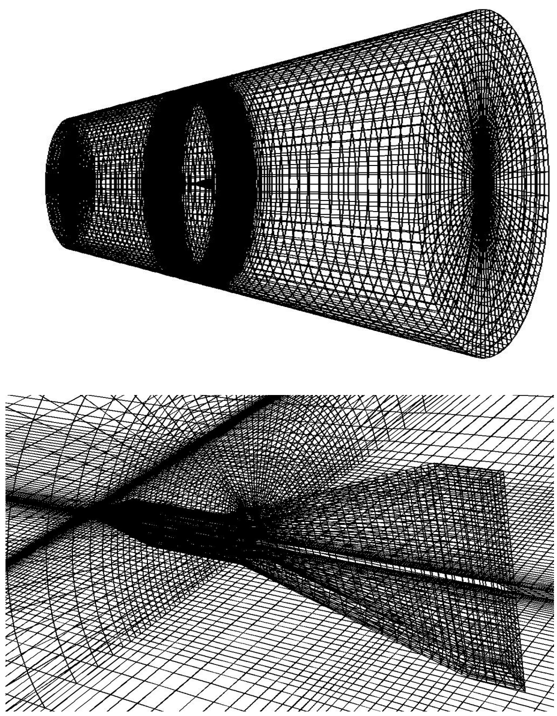

Fig. 2 Computation domain and grid system around a LEX-delta wing

Fig.2 shows the 3D grid system and computational domain used in the present study. 3D structured grid system is used to simulate the flow field of delta wing and node points are about eight hundred thousands. The calculation was carried out to provide the best mesh resolution around the wing for given number of points. The grids are clustered in the region with the flow separation which occur at the near of the surface and sharp leading edge of the delta wing so that provide more accurate predictions of the flow field. The dimension of computational domain is setup at 6 times of chord length toward upstream from the apex of the model, 15 times of

Fig. 3 Delta wing model in the test section of KAFA subsonic wind tunnel

chord length toward downstream from trailing of the model and 8 times of chord length along the spanwise. The pressure inlet boundary condition, the pressure outlet boundary condition and the far-field boundary condition are applied to the upstream boundary, downstream boundary and circumferential boundary of the computational domain, respectively. The Reynolds number based on the free stream velocity and the wing chord length was about 0.88×10^6.

Fig.3 shows the experimental model mounted in the wind tunnel test section. The off-surface visualization was made in the other KAFA small-sized low-speed wind tunnel, having a test section size of 0.9m(W) ×0.9m(H) ×2.1m(L). The turbulence intensity was less than 0.2% for the available test section speed range from 3.6m/s to 50m/s. The free stream velocity of the off-surface visualization was 6.2m/s. The corresponding Reynolds number, based on this free stream velocity and the wing centerline chord(100mm), was 4.4×10^5.

3. REULTS AND DISCUSSION

Fig.4 presents the wing upper surface static pressure distributions of the yawed LEX-delta wing on some variations in chord stations, where C_p is static pressure coefficient, defined as $C_p=(p-p_8)/?V^2/2$ and p_8 is the free stream pressure. The pressure distribution of spiral suction peak and large spanwise gradient appears at the windward side. At the 30% chord station of the delta wing, the suction peak pressure has at y/s=–0.9 (its value was –2.5). It moves abruptly toward the wing centerline (*x/c*=0.3-0.45), and has almost same position (*y/s*=0.55) according to the variations of the chord station (*x/c*=0.45-0.8). In the leeward side, the location of peak pressure decreases monotonically toward the wing centerline. The largest suction pressure peak occurred at *x/c*=0.6 is located at *y/s*=- 0.55 and its value is –3.0.

At the 60% and 80% chord stations, the wing surface pressure resumes the spiral suction peak and the large spanwise gradient in the windward side. Comparing the previous result(9) of no LEX-delta wing with these results, it can be found that the largest pressure peak was much diminished by using LEX configuration, while the pressure peaks and spanwise pressure gradients resumed according to the chordwise direction by the wing vortices developed in LEX configuration. It seems that the computational predictions well predict the experimental results qualitatively.

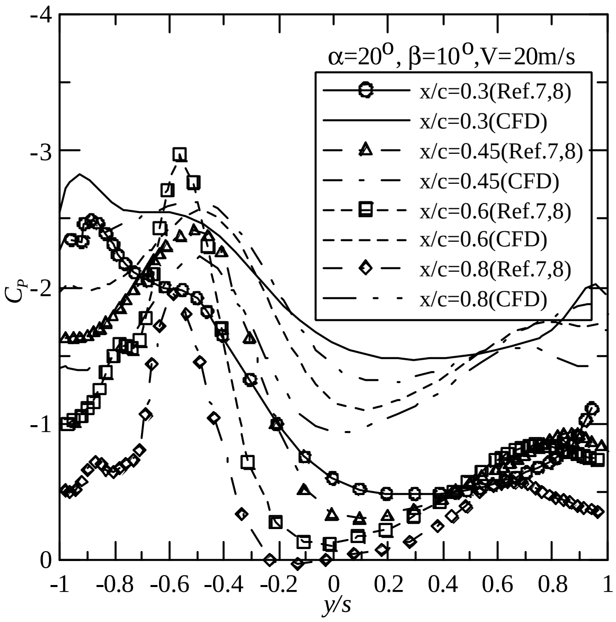

Fig. 4 Wing surface pressure distribution of the delta wings with some variations in chord stations

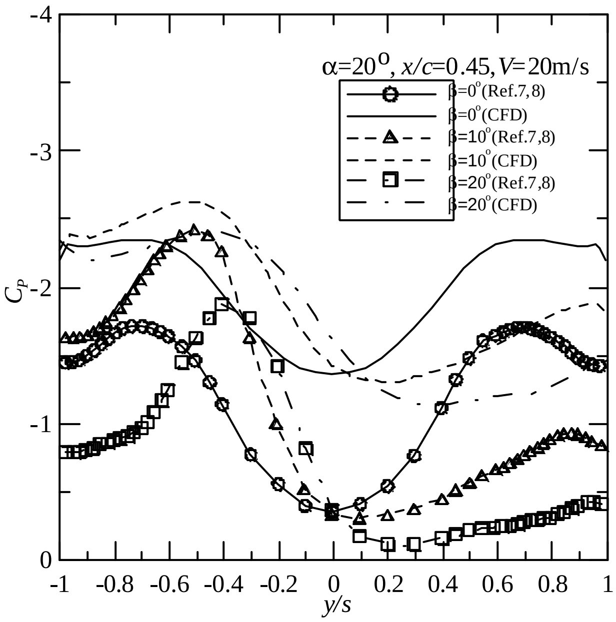

Fig. 5 Wing surface pressure distribution of the delta wing with the variations in the yaw angle

Fig.5 shows the wing surface pressure distributions of the delta wing with some variations in the yaw angle. The sharp pressure peaks of the delta wing increase and

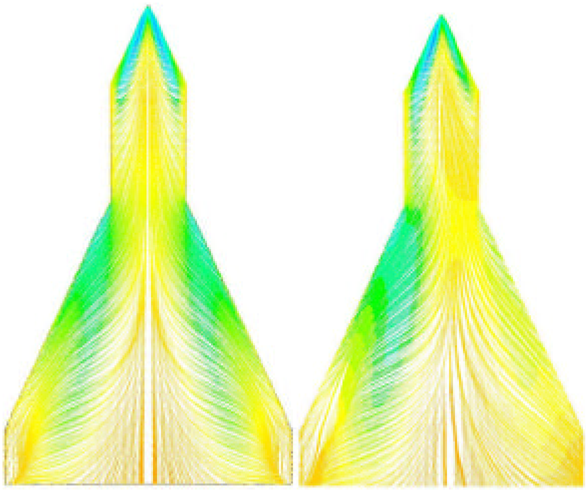

(a) *b*=0^{o} (b) *b*=10^{o}

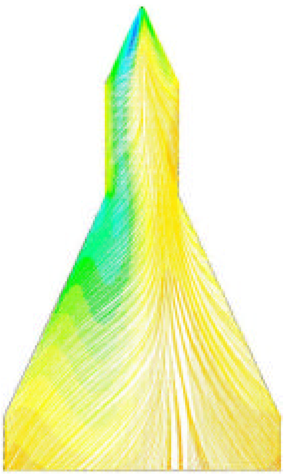

(c) *b*=20^{o}

Fig. 6 Computational oilflow with the variations in the yaw angle (a=20^{o},V=20m/s)

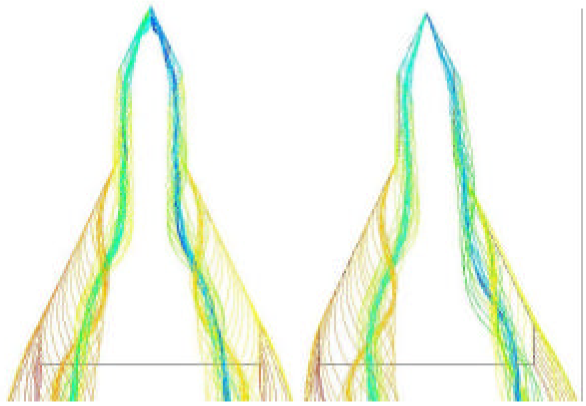

(a) *b*=0^{o} (b) *b*=10^{o}

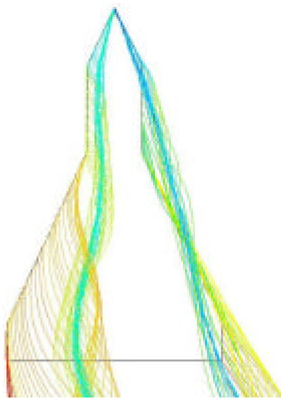

(c) *b*=20^{o}

Fig. 7 Path lines over the upper surface of the delta wing

decrease with increasing the yaw angle, and its largest value was obtained at *b*=10^{o}. As increasing in the yaw angle, it was found that the vortex breakdown appears abruptly at the leeward side of the delta wing. From the figure, it can be seen that the computational predictions well predict the experimental results qualitatively.

Fig.6 shows limited streamlines on the delta wing upper surface by using a computational oilflow method colored by static pressure. At *b*=0^{o}, it can be seen that the computational method reproduces well a typical subsonic flow field of a delta wing such as the symmetric primary or secondary vortex and its attachment. As increasing the yaw angle, the low pressure region at the leeward disappeared. From the figure, the reattachment region of primary vortex increases in the windward side relative to the leeward side with increasing *b*.

Fig.7 shows fluid particle path lines over the upper surface of the delta wings at a=20^{o}, V=20m/s. At *b*=0^{o}, it seems that the wing vortices from the LEX do not break down until reaches the trailing edge. As increasing *b*, the wing vortex flows spread out at the leeward side until reaches the trailing edge. In windward side, however, the wing vortex developed in the LEX region remains its structure up to the trailing edge of the delta wing.

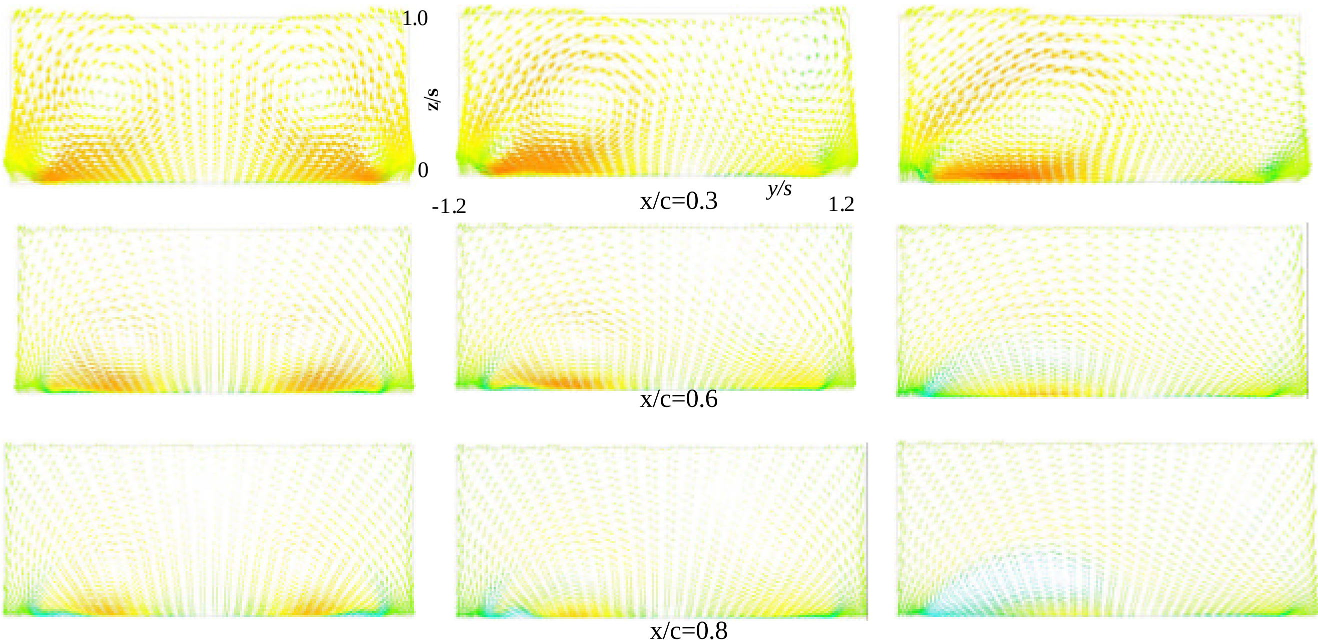

(a) b=0°　(b) b=10°　(c) b=20°

Fig. 8 Cross flow velocity vector according to chord stations (a=20°, V=20m/s)

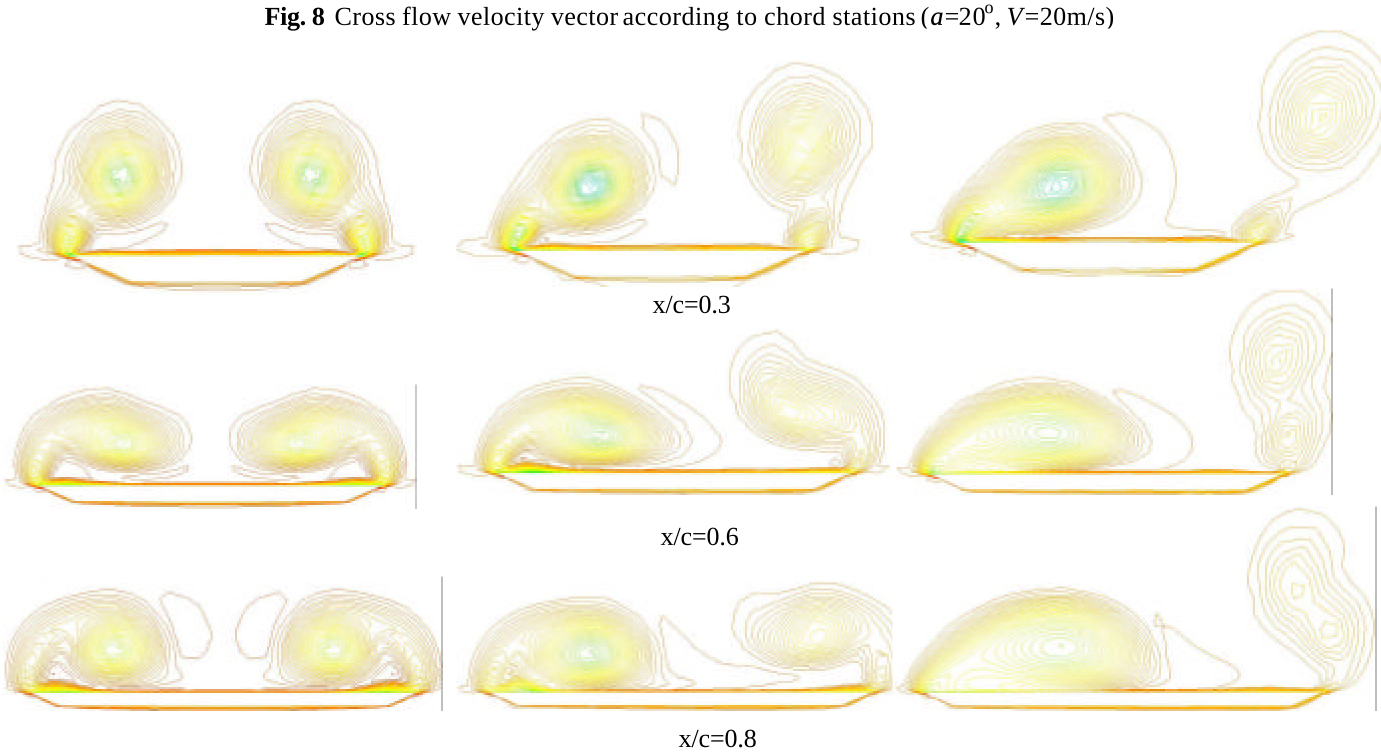

(a) b=0°　(b) b=10°　(c) b=20°

Fig. 9 Total pressure contour according to chord stations (a=20°, V=20m/s)

Fig.8 presents cross flow velocity vector for the LEX-delta wing on the vortical section of some chord stations at α=20°, V=20m/s. The LEX vortex pair at the 30% chord station is moved to inboard and downward as increasing the chord station regardless of the yaw angle. The LEX vortex of the windward side appears at each chord station and yaw angle, while its vortex of leeward side disappears as increasing the chord station and the yaw angle.

Fig.9 shows the total pressure contours at the cross-section of 30%, 60% and 80% chord stations. The total pressure coefficient is defined as $C_{pt}=(p_t-p_{t8})/q$, where p_t is the total pressure of a point, p_{t8} is the total pressure of the free stream and q is the dynamic pressure of the free stream. The total pressure coefficient in this study can be considered as the total pressure loss coefficient. It is non-dimensional property used to explain the structural characteristics of vortex flow field and the location of vortex core. At each yaw angle, the development of two vortices was observed at x/c=0.3, and the vortices were unified with increasing the chord station. Also, the location of vortex core of the LEX-delta wing is relatively attached to the wing upper surface in high chord station than in low chord station.

4. CONCLUSIONS

The basic structure, development and break down of the vortical flow field over the LEX-delta wing at high angle of attack according to the variation of the yaw angle were investigated. Three-dimensional Navier-Stokes numerical simulations were carried out to predict the complex vortex flow field characteristics, including leading edge separation, vortex breakdown. Flows over 65° sweepback angle delta wing with sharp leading edges were investigated and compared with available experimental data. As a result, the largest pressure peak appears at the windward side, while the pressure peaks and spanwise pressure gradients resumed according to the chordwise direction by the wing vortices developed in LEX configuration. Solutions obtained from this CFD visualized the flow field around the delta wings moderately and were in close agreement with the experimental measurements.

ACKNOWLEDGEMENT

The present research is sponsored by the Korean Science and Engineering Foundation(Grant Number KOSEF R01-2000-00318). The authors would like to tank KOSEF.

REFERENCES

(1) Erickson, G. E., Schreiner, J. A. and Roges, L. W., 1989, "On the Structure, Interaction, and Breakdown Characteristics of Slender Wing Vortices at Subsonic, Transonic, and Supersonic Speeds," AIAA Paper, AIAA-89-3345.

(2) Verhaagen, N. G., 1999, "Effects of Reynolds Number on the Flow over 76/40-deg Double-Delta Wings," AIAA Paper.

(3) Varhaagen, N. G. and Naarding, S. H. J., 1989, "Experimental and Numerical Investigation of Vortex Flow over a Sidesliping Delta Wing," J. of Aircraft, Vol.26, No.11, pp.971-978.

(4) Ekaterinaris, J. A. and Schifft, L.B., 1993, "Numerical Prediction of Vortical Flow over Slender Delta Wings," J. of Aircraft, Vol. 30, No. 6, pp.935-942.

(5) Kern, S. B., 1993, "Vortex Flow Control Using Fillets on a Double-Delta Wing," J. of Aircraft, Vol. 30, No. 6, pp.818-825.

(6) Ekaterinaris, J. A. and Schiff, L. B., 1990, "Numerical Simulation of the Effects of Variation of Angle of Attack and Sweep Angle on Vortex Breakdown over Delta Wings," AIAA Paper, AIAA-90-3000-CP.

(7) Sohn, M. H. and Lee, K. Y., 2001, "Observation of the Vortex Interaction over an Yawed Delta Wing with Leading Edge Extension by Flow Visualization and 5-hole Probe Measurements," Proceedings of the KSME 2001 Fall Annual Meeting(B), pp.388-393.

(8) Sohn, M. H., Lee, K. Y. and Baek, S. W., 2001, "Effect of Sideslip on the Vortex Flow over a Delta Wing with the Leading Edge Extension," Proceedings of the KSAS.

(9) Kim, T. H., Kweon, Y. H., Kim, H. D. and Sohn, M. H., 2002, "Computational Investigation of the Vortical Flow over a Yawed Delta Wing at High-Angle of Attack," Proceedings of the KSME 2002 Fall Annual Meeting(B).